

18.6

Co 52

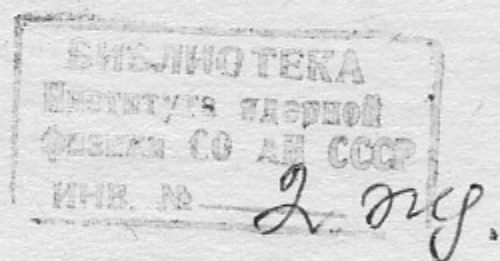
1984



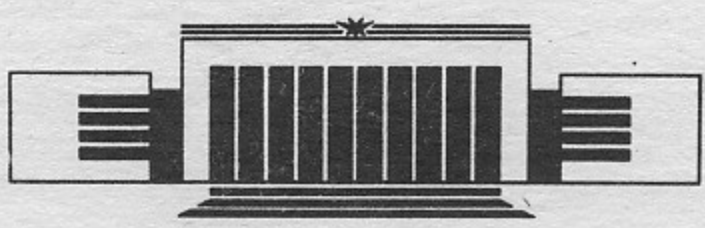
ИНСТИТУТ ЯДЕРНОЙ ФИЗИКИ СО АН СССР

B.V. Chirikov and D.L. Shepelyansky

**CHAOS BORDER
AND STATISTICAL ANOMALIES**



PREPRINT 86-174



НОВОСИБИРСК

V

Chaos Border and Statistical Anomalies^{*)}

B.V. Chirikov and D.L. Shepelyansky

Institute of Nuclear Physics
630090, Novosibirsk, USSR

A B S T R A C T

The review of authors' studies in the critical structure near a chaos border in phase space, and in its impact on the statistical properties of chaotic component is given. The phenomenon of renormalization chaos is discussed in detail. A simple resonance theory of critical phenomena in two-dimensional canonical maps is also presented.

^{*)} Report at the International workshop «Renormgroup-86», Dubna, 1986.

The dynamical chaos is the random after Alekseev (unpredictable) motion of a purely dynamic system free of any random parameters, or noise, in the equations of motion. According to the Alekseev—Brudno theorem (see Ref. [1]) the necessary and sufficient condition for such a chaos is the positive (nonzero) dynamical Kolmogorov—Sinai (KS) entropy h , that is an exponential local instability of motion (on some transitive set whose dimensionality is larger than one). Owing to that instability the concept of trajectory of a chaotic motion loses the physical meaning (just as notion of unstable equilibrium becomes purely formal), and one has to turn a statistical description of motion which is assumed to be stable. Here the main problem is to find out the statistical properties of a chaotic motion.

A distinctive feature of this problem is in that the statistical properties of the chaos are completely determined by the dynamics of a system without any additional statistical hypotheses. Moreover, that statistics may happen to be rather unusual, or «abnormal». We put here quotes as the abnormal is not the behaviour of a dynamical system itself but rather our traditional simplified conception of the latter, just due to the additional statistical hypotheses which had been required, indeed, prior to the discovery of dynamical chaos.

It was commonly assumed, for example, that the correlation of a random process in statistical mechanics decays exponentially in time. This appeared to be confirmed in the theory of dynamical chaos with its exponential local instability. Indeed, there are special, so called Anosov, systems, where the correlation decays exponentially.

Yet, generally, the decay may be a much slower one, as a power law, for example. Apparently first such a phenomenon of (correlation) «long tails» has been discovered in numerical experiments with the hard sphere model of a gas [2] (see also Refs [3]: Chapter 16, and [4]).

Below we are going to consider another, typical for oscillator systems, case of divided phase space with coexisting chaotic as well as regular components of motion. A peculiar surface separating any two of these components, the chaos border, is just the principal object of our studies.

Since long ago it has been noticed that the vicinity of chaos border has generally a very intricate structure of hierarchically interwoven domains of both chaotic and regular motions in a wide range of spatial and temporal scales (see, e. g., Ref. [5]; an example of a simple chaos border is presented in Ref. [4]).

The detailed studies, which basic results are outlined below, revealed that just such a complicated structure of the «edge» of a motion chaotic component results in statistical «anomalies». In fact, only the simplest class of such dynamical systems has been investigated up to now, those with minimal dimensionality when the dynamical chaos is still possible. These are conservative Hamiltonian systems of two freedoms, and the related two-dimensional canonical mappings. In the latter case the chaos border is just a curve.

One interesting result of the studies of chaos border was the discovery of a new type of dynamical chaos, which we term the *renormalization chaos*, i. e. chaotic fluctuations of the whole phase plane structure near the border upon transition from one space-time scale to another one.

1. MODEL

As a model we have chosen separatrix map [5, 6] specified by the equations:

$$\bar{z} = z + \sin x; \quad \bar{x} = x - \lambda \ln |\bar{z}|; \quad (1.1)$$

where z, x are action-phase variables, and λ —the parameter. Particularly, this map describes a chaotic layer around the perturbation splitted separatrix of a nonlinear resonance [5].

Model (1.1) is reduced, locally in z , to the standard map [5, 6]:

$$\bar{y} = y + K \cdot \sin x; \quad \bar{x} = x + \bar{y}, \quad (1.2)$$

where new action $y = \lambda(z_1 - z)/z_1 - \lambda \ln |z_1|$, and new parameter $K = -\lambda/z_1$. As the latter map is periodic in y there exists the critical $|K| = K_g \approx 1$ separating bounded ($|K| \leq K_g$) and unbounded ($|K| > K_g$) motion in y (see Section 3 below). This approximately determines two borders of the main chaotic component

$$|z_b| \approx \lambda, \quad (1.3)$$

which fills up the layer $|z| \leq \lambda$. Outside this region there are also other isolated chaotic layers, generally of a considerably smaller width, about the separatrices of various resonances, for example, at z_n satisfying $\lambda \cdot \ln |z_n| = 2\pi n$ where integer $n \geq \lambda \cdot \ln \lambda / 2\pi$.

Inside the main chaotic component the domains of stable motion are embedded, corresponding to the centers of some resonances. Hence, the main chaotic component has not only external borders (1.3) but also a host of internal ones surrounding the stable domains. Near any of these borders the phase plane structure becomes highly intricate while the share of stable components amounts up to 50 per cent. It was observed a long time ago that a trajectory may «stick» within those domains for a long time (see, e. g., Ref. [5]) which leads to a substantial change in the statistical properties of the motion in chaotic component. It is just the subject of our studies in question which have been started in 1981 (see Ref. [7]).

Notice, that the chaotic component in model (1.2) has positive KS-entropy $h \approx \ln(K/2)$, $K > 4$ (see Ref. [5]), hence in the chaotic layer of model (1.1) $h > 0$, too.

2. STATISTICS OF THE POINCARÉ'S RECURRENCES

One of the most important statistical properties of motion is the temporal correlation. However, our experience taught us that the most simple and reliable statistical characteristic to measure is another one, the temporal distribution of Poincaré's recurrences. To this end we numerically calculated time τ (the number of iterations for map (1.1)) between successive crossing of line $z=0$ by a trajectory, i. e. the transition time from one half of the chaotic layer into another one. Both halves are symmetric up to a shift in phase: $x \rightarrow x + \pi$. The basic result of this measurement was integral recur-

rence probability $P(\tau)$ defined as the ratio of the number of recurrences after time τ to the total number of recurrences. Apparently first such a method was used, implicitly, in Ref. [8].

Our main results [7] are presented in Fig. 1 taken from Ref. [7]. Two qualitatively different regions of dependence $P(\tau)$ are clearly seen. At small τ the numerical data are well described by the function $P(\tau) = \tau^{-1/2}$. It is in agreement with the results of Ref. [8] where also the chaotic layer of a nonlinear resonance was actually studied. This dependence has a simple physical meaning: it corresponds to a homogeneous diffusion within the layer $|z| \leq \lambda$ during the time interval $\tau_0 \sim \lambda^2$.

The second region ($\tau > \tau_0$) is much more interesting and rich. Dependence $P(\tau)$ here has two distinctive features. First, it is a power law, at average in τ :

$$P(\tau) \approx \frac{A(\lambda)}{\tau^p}, \quad (2.1)$$

the exponent p weakly depending on λ with the mean value over all the data in Fig. 1

$$\langle p \rangle = 1.45. \quad (2.2)$$

Second, there are irregular oscillations of the local exponent $\bar{p} = d \log P / d \log \tau$ which, however, have nothing to do with fluctuations of the chaotic motion as they do not depend on the initial conditions. In other words, statistics $P(\tau)$ proves to be the same for completely different (due to local instability) trajectories. This would imply that both the oscillations and average power law dependence $P(\tau)$ describe the structure of the chaotic layer edge, i. e. of the chaos border.

The statistics of recurrences is closely related to the temporal correlation decay for chaotic motion within the layer. Indeed, the mean relative sojourn («sticking») time for a trajectory in some neighbourhood of the chaos border is of the order $\tau P(\tau) / \langle \tau \rangle$ where $\langle \tau \rangle \approx 3\lambda$ is the average recurrence time [7]. From the ergodicity of motion this time is equal to the relative measure $\mu(\tau)$ of the sticking domain which is just the residual correlation. A detailed calculation of the correlation from statistics of recurrences is given in Ref. [9] (see also Fig. 2). We obtain

$$C(\tau) \sim \mu(\tau) \sim \frac{\tau P(\tau)}{\langle \tau \rangle} \sim \frac{1}{\tau^p}; \quad p_c = p - 1. \quad (2.3)$$

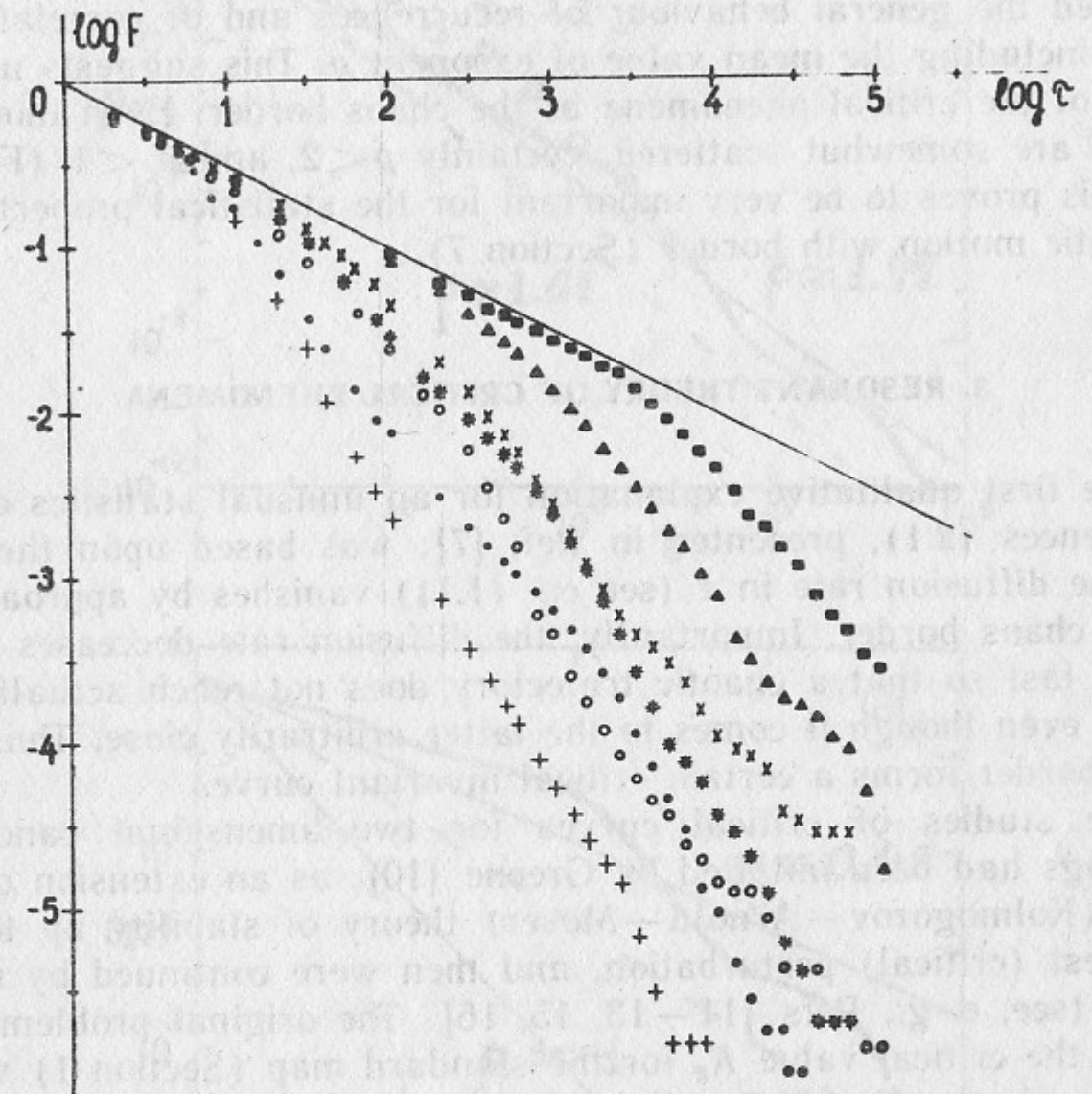


Fig. 1. Distribution of Poincaré's recurrences in the chaotic layer of map (1.1): 10^7 iterations for each $\lambda=1$ (+); 3 (\cdot); 5 (\circ); 7 ($*$); 10 (\times); 30 (\blacktriangle); and 100 (\blacksquare); the straight line is $P(\tau) = \tau^{-1/2}$.

In Fig. 2 the comparison is given of our data with those in Ref. [9] obtained in a unique run of 1600 trajectories by 2×10^8 iterations each! In spite of a different two-dimensional canonical map explored the general behaviour of recurrences and of correlation is close, including the mean value of exponent p . This suggests universality of the critical phenomena at the chaos border. Even though p values are somewhat scattered, certainly $p < 2$, and $p_c < 1$ (Figs 1, 2). This proves to be very important for the statistical properties of a chaotic motion with border (Section 7).

3. RESONANT THEORY OF CRITICAL PHENOMENA

The first qualitative explanation for an unusual statistics of the recurrences (2.1), presented in Ref. [7], was based upon the idea that the diffusion rate in z (see eq. (1.1)) vanishes by approaching to the chaos border. Importantly, the diffusion rate decreases sufficiently fast so that a chaotic trajectory does not reach actually the border even though it comes to the latter arbitrarily close. Thus, the chaos border forms a certain critical invariant curve.

The studies of critical curves for two-dimensional canonical mappings had been initiated by Greene [10], as an extension of the K.A.M (Kolmogorov—Arnold—Moser) theory of stability up to the strongest (critical) perturbation, and then were continued by many others (see, e. g., Refs [11—13, 15, 16]). The original problem was to find the critical value K_g for the standard map (Section 1) which corresponds to the destruction of the last (strongest) invariant curve. Greene conjectured that this curve has the rotation number

$$r = r_G = (1, 1, \dots, 1, \dots) = \frac{\sqrt{5} - 1}{2} = 0.618\dots$$

where

$$r = \frac{\langle \omega \rangle}{2\pi} = \frac{1}{2\pi} \lim_{n \rightarrow \infty} \frac{x_n - x_0}{n} \quad (3.1)$$

and the integers in brackets are the elements of the continued fraction expansion for r . Irrational r_G is called the «Golden Mean» and is known to have the worst approximation by the rational convergents. The latter was precisely the idea of Greene's conjecture. Using a special numerical procedure, which proved to be highly effi-

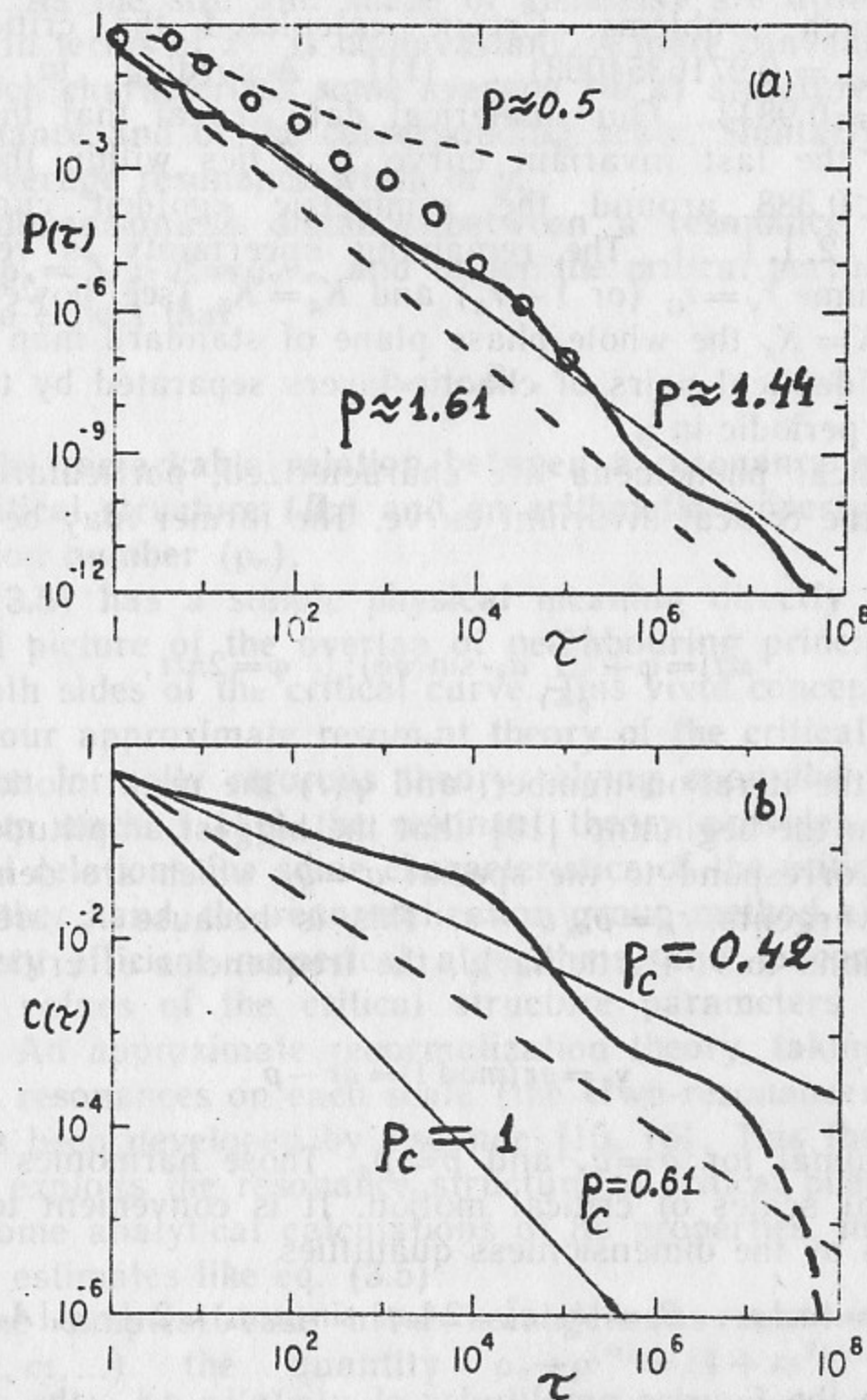


Fig. 2. Statistical properties of motion with chaos border: *a*—Poincaré's recurrences; *b*—correlation decay. Curves are Karney's numerical data [9]; circles present our data for model (1.1), $\lambda=3$. Straight lines indicate power law with the exponent shown.

cient in such problems, Greene calculated the critical value $K_c(r_G) = K_G = 0.97163540631\dots$ [11]. According to Ref. [14] $K_g < 63/64 = 0.9843\dots$. Our numerical data reveal that the rotation number of the last invariant curve (r_g) lies within the interval $0.380 < r_g < 0.388$ around the symmetric «golden curve» with $r = 1 - r_g = (2, 1, 1, \dots)$. The remaining uncertainty is very small, and we assume $r_g = r_G$ (or $1 - r_g$) and $K_g = K_G$ (see, however, Section 5). At $K = K_g$ the whole phase plane of standard map is decomposed into identical pairs of chaotic layers separated by the critical curves and periodic in y .

The critical phenomena are characterized, particularly, by the motion on the critical invariant curve. The former may be described as [12]:

$$x(t) = \varphi + \sum_{q=1}^{\infty} a_q \cdot \sin(q\varphi); \quad \varphi = 2\pi r t, \quad (3.2)$$

where t is the iteration number, and $\varphi(t)$ the mean motion. It was noticed from the beginning [10] that the biggest amplitudes A_q (see eq. (3.4)) correspond to the special $q = q_n$ which are denominators of the convergents $r_n = p_n/q_n \rightarrow r$. This is because r_n are the best approximations to r . Particularly, the frequencies of critical motion (3.2)

$$v_q = qr \pmod{1} = qr - p \quad (3.3)$$

become minimal for $q = q_n$ and $p = p_n$. Those harmonics determine the principal scales of critical motion. It is convenient to describe these scales by the dimensionless quantities

$$A_n = |a_n| q_n; \quad B_n = |b_n| q_n^2 = 2A_n q_n \sin(\pi r q_n) \approx 2\pi |v_n q_n| A_n. \quad (3.4)$$

Here b_n are the Fourier amplitudes of $y(\varphi)$; $|v_n q_n|$ — the dimensionless frequencies, and the relation of B_n to A_n is obtained from the second eq. (1.2) and eq. (3.2), the last expression for B_n holding under $q_n \gg 1$.

Critical motion (3.2) represents to some extent the structure of its close neighbourhood, too. Particularly, the principal scales correspond to strongest resonances $r_n = p_n/q_n$ which are at distance (in frequency) $\Delta r_n = r - r_n = v_n/q_n$ off the critical curve. Each resonance forms a chain of q_n stable «islands». Hence, its characteristic x scale is $2\pi/q_n$, and one may introduce a dimensionless variable

$x^{(n)} = x q_n$. As the size and shape of «islands» are different the description in terms of $\tilde{x}^{(n)}$ is noninvariant. A more convenient quantity is A_n which characterizes some average (in x) structure of a principal resonance and of the corresponding scale. Similarly, B_n describes the average resonance width in y .

The dimensionless distance between a resonance and critical curve is $\rho_n = \Delta r_n \cdot q_n^2 = q_n v_n$, and under the critical perturbation, it is natural to expect that

$$\rho_n \sim B_n. \quad (3.5)$$

This is the remarkable relation between a resonance characteristic of the critical structure (B_n) and an arithmetic property of the critical rotation number (ρ_n).

Eq. (3.5) has a simple physical meaning directly related to a graphical picture of the overlap of neighbouring principal resonances at both sides of the critical curve. This vivid conception forms a basis of our approximate resonant theory of the critical phenomena. Unlike the formally rigorous theory relying upon the renormalization group method [11] the resonant theory provides approximate analytical relations for some characteristics of the critical structure. On the other hand, the renormalization group method allows to construct very efficient numerical algorithms, and to compute highly accurate values of the critical structure parameters like K_G , for example. An approximate renormalization theory, taking account of only two resonances on each scale (the «two-resonance» approximation) has been developed by Escande [15, 16]. This theory also essentially exploits the resonance structure of critical phenomena, and allows some analytical calculations of its properties, more accurate than our estimates like eq. (3.5).

In the simplest case of a homogeneous continuous fraction $r^{(m)} = (m, m, \dots)$ the quantity $\rho_n \rightarrow \rho^{(m)} = (4 + m^2)^{-1/2}$. Hence, $B_n \rightarrow B^{(m)}$, and $A_n \rightarrow A^{(m)}$ also. In a particular case $m = 1$, $r = r_G$, which has been studied in detail, according to our numerical data

$$A^{(1)} = 0.16736\dots; \quad B^{(1)} = 0.47027\dots; \quad \frac{B^{(1)}}{\rho^{(1)}} = 1.0515\dots \quad (3.6)$$

The value of $A^{(1)}$ is two times of the result in Ref. [12] due to a different normalization of amplitudes a_n there which holds for a periodic trajectory only.

The critical structure is also characterized by various scaling

factors, e. g., $s_x^{(n)} = \tilde{x}^{(n+1)}/\tilde{x}^{(n)} = q_{n+1}/q_n \equiv s^{(n)}$ where the latter is a purely arithmetical factor. For $r=r_G$ the factor $s^{(n)} \rightarrow s = 1/r_G$ that is the exact scale invariance holds in the limit $n \rightarrow \infty$. Similarly, $s_y^{(n)} = (q_{n+1}/q_n)^2 = (s^{(n)})^2$, and $s_y = s^2$. Whence, for the area, or measure $s_\mu \approx s_x s_y = s^3$ [17]. This relation is only approximate as s_x, s_y describe the average scale ratios over the critical curve. According to numerical data in Ref. [11], on the dominant symmetry line ($x=\pi$) the factors $s_x(\pi) = 1.414836062\dots$; $s_y(\pi) = 3.066888246\dots$ which are quite different from the mean values $s = 1.618\dots$, and $s^2 = 2.618\dots$. However, numerical value $s_\mu = 4.339144088\dots$, which remains constant along the curve due to measure conservation, is fairly close to $s^3 = 4.236\dots$. It was confirmed recently in Refs [15, 18] using the two-resonance theory.

We also studied numerically the convergence $A_n \rightarrow A^{(1)}$, and have found two characteristic rates:

$$\frac{|A_n - A^{(1)}|}{A^{(1)}} \approx \left| \frac{0.23}{q_n^2} - \frac{0.11}{q_n} \right|. \quad (3.7)$$

The first, rapid, rate relates to the arithmetics: $|\sqrt{5}v_n|q_n - 1| = 1/5q_n^2$. The slower convergence was interpreted earlier [19] as the effect of a certain local perturbation. However, according to Ref. [15], the convergence $\sim q_n^{-1}$ naturally arises from the renormalization group equations. Thus, the question of the local perturbation remains open (see Section 6 below).

At a small difference $|K - K_G|$ the behaviour of the principal dimensionless amplitudes is described by the following approximate empirical expression:

$$A_n = A^{(1)} \cdot \exp[1.2 q_n (K - K_G)], \quad (3.8)$$

which improves the relation due to Escande (see Ref. [12]). Numerical data in Ref. [12] show that near the critical value the exponent in eq. (3.8) depends linearly on K . This expression holds for sufficiently large q_n when the deviation (3.7) from the asymptotic value can be neglected.

In the subcritical case ($K < K_G$) the amplitudes decay exponentially, like in the KAM theory for a typical analytic perturbation [20]. At any $K > K_G$ the amplitudes grow exponentially, and a continuous invariant curve with $r=r_G$ gets destroyed and is transformed into some nowhere dense invariant Cantor set, the so called *cantorus* [13]. All resonances with $q_n \geq (K - K_G)^{-1}$ are completely

destroyed, and form a solid chaotic layer. Its width (in frequency) Δr_s is terminated by the principal undestroyed resonance with minimal $q_n^* \sim (K - K_G)^{-1}$:

$$\Delta r_s \sim (q_n^*)^{-2} \sim (K - K_G)^2. \quad (3.9)$$

Numerical simulation shows that for $q_n \geq q_n^*$ the exponential growth (3.8) is saturated so that $A_n \sim 1$.

Other dimensionless quantities characterizing the neighbourhood of a critical curve behave in a similar way, for example, Greene's residue R_n [10] whose value determines the stability of periodic trajectories $r_n = p_n/q_n$:

$$R_n = \sin^2\left(\frac{q_n \Omega_n}{2}\right). \quad (3.10)$$

Here Ω_n is the frequency of small oscillations about that trajectory, the stability corresponding to the interval: $0 < R_n < 1$. According to Ref. [11] $R_n \rightarrow R^{(1)} = 0.2500888\dots$ at $K = K_G$ which implies that the resonance centres remain undestroyed. For $K \neq K_G$ the dependence $R(K)$ is somewhat different from eq. (3.8):

$$R_n = R^{(1)} \exp[1.20 q_n^{1+\varepsilon} (K - K_G)] \quad (3.11)$$

with $\varepsilon = 0.013$ [11]. Besides, for $\Delta K = K - K_G > 0$ the residues grow with n indefinitely. It has a simple physical meaning, namely, the Lyapunov exponent $\lambda_n \approx \ln(4R_n)/q_n$ remains approximately constant, and is close to the entropy $h \sim \Delta K$ in the critical chaotic layer.

4. RENORMALIZATION CHAOS

The renormalization group, which describes a critical structure, may be considered as some abstract dynamical system in a space of two-dimensional canonical maps determining the motion structure in dimensionless variables. The serial number of a principal scale of the critical structure, which is proportional to the logarithm of a characteristic space or time scale, plays here the role of dynamical time, the so called «renormalization time».

In case of a homogeneous continuous fraction for the rotation number the critical structure is characterized by the exact scale invariance. It corresponds to the simplest renormalization dynamics, a

fixed point. Naturally, a question arises about a more complicated renormalization group. One may consider, for instance, periodic continued fractions. These are reduced, however, again to a fixed point of the corresponding power of renormalization map.

The chaotic renormalization dynamics, predicted in Ref. [21], and demonstrated in Ref. [19], appears to be much more interesting. A similar phenomenon was independently studied also in Ref. [22] for a one-dimensional mapping. The renormalization chaos occurs when the sequence of a continuous fraction elements $\{m_n\}$ is random, and this is just the case for almost any irrational r [23]. Indeed, m_n are given by the Gauss map

$$r_{n+1} = \frac{1}{r_n} \bmod 1; \quad m_{n+1} = \left[\frac{1}{r_n} \right] \quad (4.1)$$

with initial $r_0 = r$. Homogeneous continuous fractions are the particular case with the special initial condition $r_0 = r^{(m)}$. Map (4.1) has a positive entropy $h = \pi^2/6 \ln 2$.

The randomness of sequences $\{r_n\}$ and $\{m_n\}$ results in randomness of all the other parameters of a critical structure. For example, the main scaling factor $s_n = q_{n+1}/q_n = 1/\omega_{n+1}$ is described also by Gauss' map:

$$\omega_n = \frac{1}{\omega_{n+1}} \bmod 1 \quad (4.2)$$

backwards in renormalization time with the «initial» value $\omega_\infty = \tilde{r}$ where \tilde{r} is the irrational with reversed sequence of elements in regard to r . The frequency ratio at neighbouring scales $u_n = -v_n/v_{n-1}$ (> 0) also satisfies map (4.1) with $u_0 = r$.

The mean scaling factor for a typical r may be obtained from the steady-state distribution of map (4.2), and is equal [23]

$$\langle s \rangle = e^{h/2} \approx 3.28. \quad (4.3)$$

It is about twice as large as that for r_G .

An example of renormalization chaos is standard map for $r_b = (2111212111211121\dots) = 0.37966453\dots$ is given in Fig. 3. The choice for r_b will be explained below (Section 5). The critical value $K_c(r_b) = 0.9618704\dots$. In Fig. 3 the critical structure is represented by two dimensionless quantities, $A_n = a_n q_n$ and R_n . The values of A_n were obtained from a periodic trajectory of $q_N = 10612$ ($|r_N - r_b| \sim 10^{-8}$). Big irregular oscillations of both A_n and B_n de-

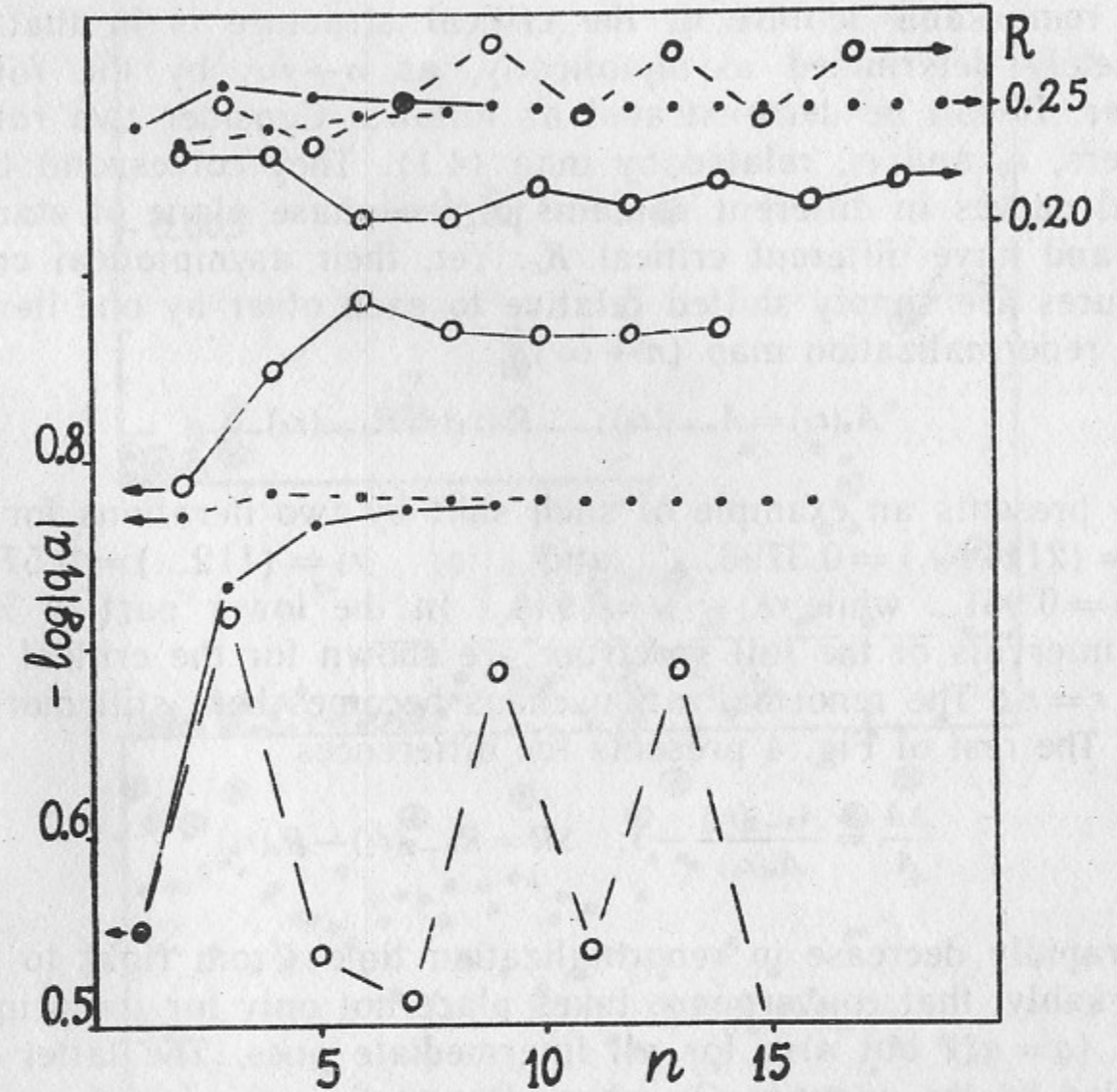


Fig. 3. An example of renormalization chaos on critical curve with $r=r_b$ (see the text) in standard map (circles). Arrows indicate correspondingly scale for $aq=A$ (the lower part) and for R in the upper part; n is renormalization time (the number of a principal scale). For comparison, the same data are given for $r=r_G$ which illustrate exact scale invariance (points).

monstrate chaotic fluctuations of the motion structure over a range of scales. Same data for $r=r_G$ (the scale invariance) are given for comparison.

A remarkable feature of the critical structure is in that it is completely determined asymptotically, as $n \rightarrow \infty$, by the rotation number. It can be demonstrated as follows. Consider two rotation numbers, r_0 and r_1 , related by map (4.1). They correspond to the critical curves in different domains of the phase plane of standard map, and have different critical K_c . Yet, their asymptotical critical structures are simply shifted relative to each other by one iteration of the renormalization map ($n \rightarrow \infty$):

$$A_n(r_1) = A_{n+1}(r_0); \quad R_n(r_1) = R_{n+1}(r_0). \quad (4.4)$$

Fig. 4 presents an example of such shift by two iterations for $r_0 = r_b = (21112\dots) = 0.3796\dots$, and for $r_2 = (112\dots) = 0.5775\dots$; $K_c(r_0) = 0.961\dots$ while $K_c(r_2) = 0.948\dots$. In the lower part of Fig. 4 some intervals of the full spectrum are shown for the critical motion at $r=r_b$. The renormalization chaos becomes here still more obvious. The rest of Fig. 4 presents the differences

$$\frac{\Delta A}{A} = \frac{A_{n-2}(r_2)}{A_n(r_b)} - 1; \quad \Delta R = R_{n-2}(r_2) - R_n(r_b). \quad (4.5)$$

Both rapidly decrease in renormalization time (from right to left). Remarkably, that convergence takes place not only for the principal scales ($q=q_n$) but also for all intermediate ones. The latter were identified by the quantity Q_v where Q was the period of the trajectory used in calculating the Fourier spectrum. Significantly, the Q values for r_b and r_2 are quite different, namely, $Q(r_b) = 10612$ while $Q(r_2) = 2554$, their ratio being $4.15505\dots$. The same is true for the q values determining dimensionless amplitudes $A=aq$. Nevertheless, the latter prove to be equal to the accuracy $\sim 10^{-3}$, and so do Greene's residues which characterize a neighbourhood of the critical curve.

Moreover, if we take a different map (1.1) and consider the critical curve with the same rotation number r_b , for which critical $\lambda_c \approx 2.57235$, the Fourier spectrum of critical motion was found to converge to the same renormalization attractor with the accuracy $|\Delta A/A| \sim 10^{-3}$.

All this evidence leads to the conclusion that in the limit $n \rightarrow \infty$ the critical structure in both cases is the same. In other words, the

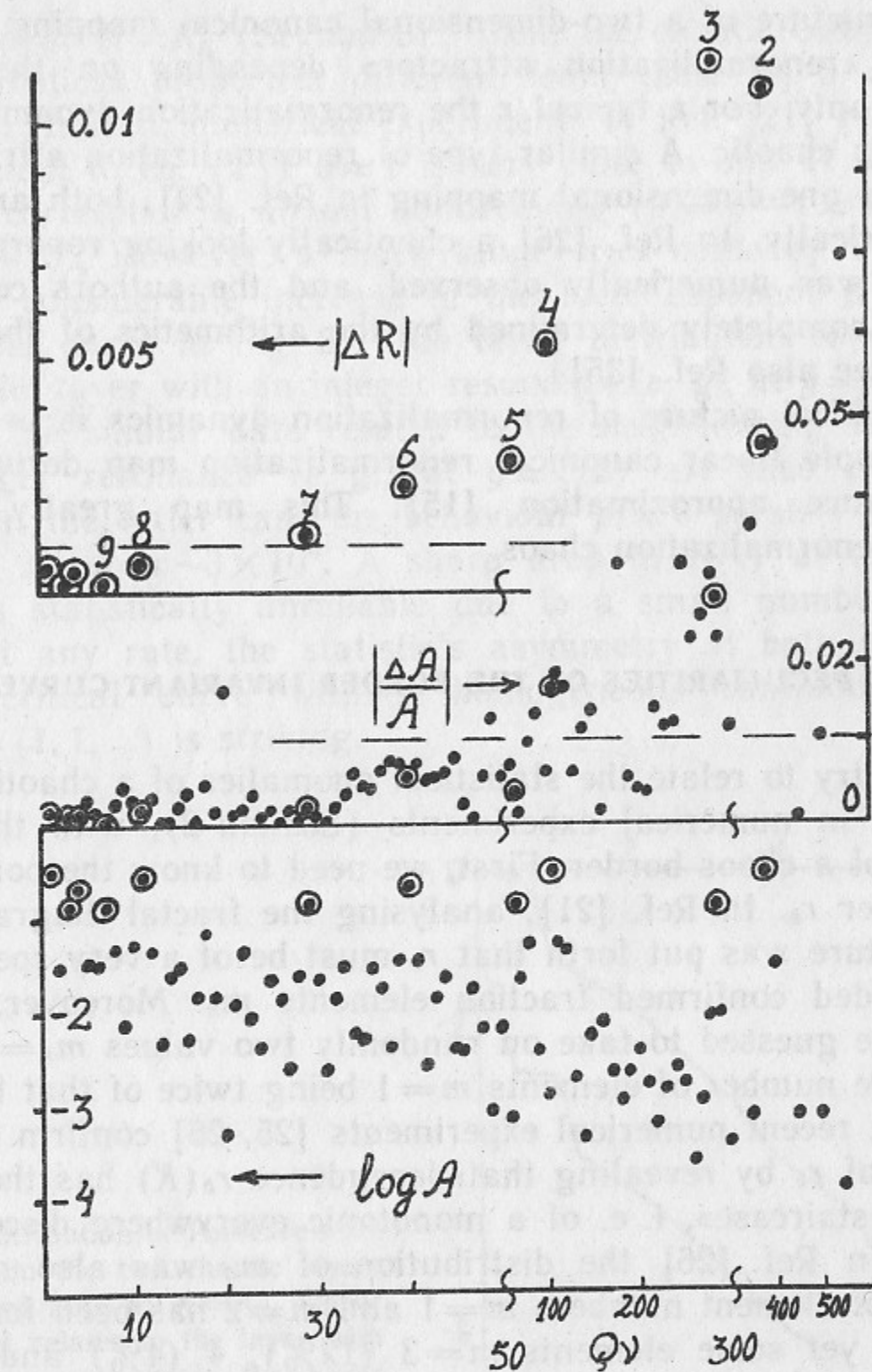


Fig. 4. Chaotic «renormalization attractor» in standard map (see the text). Arrows show the related scales. Notice changes in scale along Q_v axis. Numbers at upper points are the values of renormalization time n . The principal scales are marked by circles.

critical structure of a two-dimensional canonical mapping has some universal «renormalization attractor» depending on the rotation number r only. For a typical r the renormalization dynamics on the attractor is chaotic. A similar type of renormalization attractor was studied for one-dimensional mapping in Ref. [24], both analytically and numerically. In Ref. [26] a chaotically looking renormalization dynamics was numerically observed, and the authors conjectured that it is completely determined by the arithmetics of the rotation number (see also Ref. [35]).

A graphical picture of renormalization dynamics is provided by a very simple linear canonical renormalization map derived in the two-resonance approximation [15]. This map greatly facilitates studying renormalization chaos.

5. PECULIARITIES OF THE BORDER INVARIANT CURVE

Let us try to relate the statistical anomalies of a chaotic motion, discovered in numerical experiments (Section 2), with the critical structure of a chaos border. First, we need to know the border rotation number r_b . In Ref. [21], analysing the fractal diagram $K_c(r)$, the conjecture was put forth that r_b must be of a very special form with bounded confirmed fraction elements m_n . Moreover, the elements were guessed to take on randomly two values $m_n=1; 2$ only, the average number of elements $m=1$ being twice of that for $m=2$.

Indeed, recent numerical experiments [25, 26] confirm the special nature of r_b by revealing that dependence $r_b(K)$ has the form of a «devil's staircase», i. e. of a monotonic everywhere discontinuous function. In Ref. [26] the distribution of m_n was also measured. The ratio of element numbers $m=1$ and $m=2$ has been found to be about 2.5, yet some elements $m=3$ (12%), 4 (4%) and 5 (1%) were also observed. Besides, some asymmetry of the m_n distribution was found depending on whether n was even or odd. The asymmetry has a simple physical meaning, namely, detuning $|r_b - r_n|$ is at average less at the chaotic side of the critical curve. That asymmetry seems to be quite natural for *chaos-order* transition (see Ref. [27]).

However, a different type of the chaos border is also possible, for the *chaos-chaos* transition. Here the border invariant curve separates two different chaotic components. This is just the case in stan-

dard map at $K=K_g$ (Section 3). Then, the chaotic component may have statistical properties different from those at a chaos-order transition. Indeed, numerical experiments in Ref. [21] revealed that the exponent in eq. (2.1) $p \approx 1$ is very close to one. It would imply that the correlation is almost nondecaying ($p_c = p - 1 \approx 0$), at least, up to $\tau \sim 10^5$. However, a much longer run made by Vivaldi [28] shows a considerable increase in the local exponent \bar{p} for $\tau \geq 10^5$ (see upper curve in Fig. 5). The latter distribution corresponds to the chaotic layer with an integer resonance, e. g., at $y=0$. For comparison, the similar data related to the neighbouring layer with a half-integer resonance (e. g., at $y \approx 1/2$) are also presented in Fig. 5. In the latter case the behaviour $p_c \approx 0$ persists still longer at least, up to $\tau \sim 3 \times 10^6$. A sharp drop in $P(\tau)$ at the last two points is statistically unreliable due to a small number of events there. At any rate, the statistic's asymmetry at both sides of the border critical curve with a homogeneous continuous fraction $r_b = r_G = (1, 1, \dots)$ is striking.

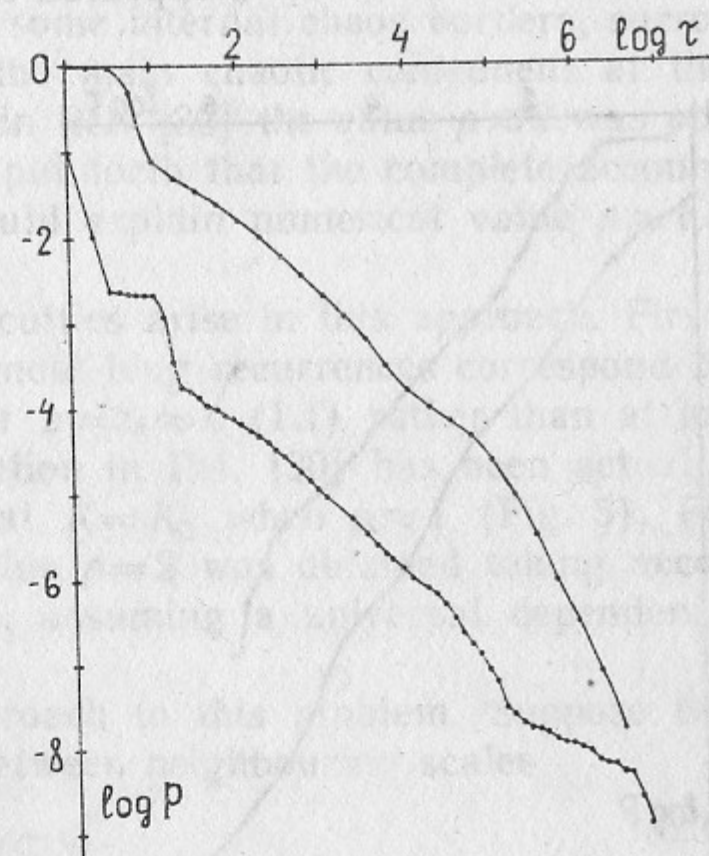


Fig. 5. Distribution of Poincaré's recurrences in the two chaotic layers of standard map at $K=K_G$. Upper curve [28] relates to the layer with integer resonance while the lower one does so to that with half-integer resonance and is shifted by $\Delta \log P = -1$. $P(\tau)$ oscillation at small $\tau \leq 10$ is due to stable regions around resonance centers.

The cause of this asymmetry, as well as of a superslow correlation decay is presently unclear. The simplest explanation would be in that the dependence $P(\tau)$ in Fig. 5 has not yet reached the asymptotic scale invariance (cf. Fig. 3). The point is that for

$P \sim \tau^{-1}$ the measure $\mu \sim \tau P(\tau)$ is almost constant according to eq. (2.3) (actually $\langle \tau \rangle \sim \ln T$ where T is the total motion time).

Another possible explanation is in that $K_g > K_G$ (Section 3), and the last invariant curve has $r_g < r_G$, i. e., is shifted toward the half-integer resonance. Extending Greene's hypothesis (Section 4) we conjecture that r_b values at the chaos-chaos transition, particularly, r_g for the standard map, are the so called Markov numbers (see, e. g., Ref. [29]). Those form denumerable set of irrationals $r^{(M)}$ with nonrandom sequence of elements $m_n = 1; 2$. These and only these numbers have minimal asymptotic detunings $\rho^{(M)} = M[(3M)^2 - 4]^{-1/2}$, with some integers M , which are all different from each other (see eq. (3.5)).

Another important question is whether the statistical properties are completely determining by the boundary rotation number r_b as is the critical structure (Fig. 4)? It is also not clear thus far. In Fig. 6 the recurrences in model (1.1) are shown for $r_b = r_G \pmod{1}$. The exponent $\rho \approx 1.4$ has a usual value (lower curve, Ref. [28]). However, the recurrences in some chaotic layer at the other side of the same critical curve r_b appeared to be anomalous with $\rho \approx 1.1$.

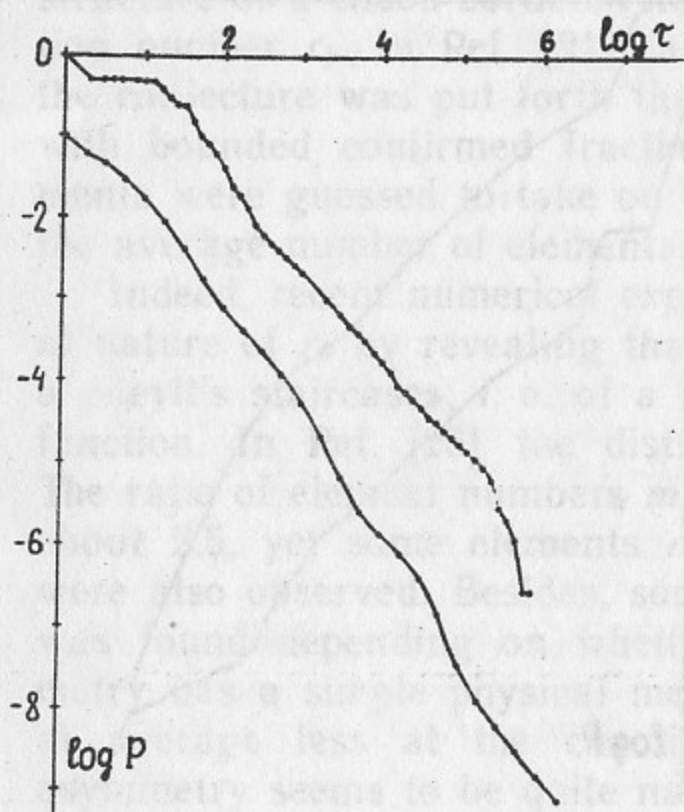


Fig. 6. The same as in Fig. 5 for separatrix map (1.1): $\lambda = 3.1819316$; $r_b = r_G$. The lower curve, shifted by $\Delta \log P = -1$, is the recurrences in the main chaotic layer, $\rho \approx 1.4$, Ref. [28]. The upper curve is the recurrences in some chaotic layer at the other side of the same critical curve.

6. POSSIBLE MECHANISMS OF STATISTICAL ANOMALIES

The simplest quantitative conjecture for the trajectory «sticking» near a chaos border is in that the transition time (τ_n) from one scale to the next is of the order of a characteristic time for a given scale (t_n):

$$\tau_n \sim t_n \sim q_n. \quad (6.1)$$

As t_n rapidly drops with n ($t_n/t_{n-2} \sim s^2$) the total sticking time $\tau \sim \tau_n$. On the other hand, the measure of all the scales $\geq n$, up to the critical curve, is $\mu \sim \mu_n \sim q_n^{-2}$ (Section 3). Hence (see eq. (2.3)) the correlation

$$C(\tau) \sim \mu(\tau) \sim \tau^{-2}. \quad (6.2)$$

Whence $\rho_c = 2$; $\rho = 3$ which certainly contradicts with the numerical results [7, 9, 21] (see Figs 1, 2, 5). Estimate (6.2) had been obtained in Ref. [17], and was confirmed by more accurate calculations in Ref. [27]. Taking account of some internal chaos borders, surrounding stable domains inside the main chaotic component at the centers of principal resonances, in Ref. [30] the value $\rho \approx 2$ was obtained, and the conjecture was put forth that the complete account for all the internal borders would explain numerical value $\rho \approx 1.5$ (2.2).

However, the following difficulties arise in this approach. First, our observations revealed that most long recurrences correspond to sticking just at the main border $z = z_b \approx \lambda$ (1.1) rather than at internal ones. Second, the calculation in Ref. [30] has been actually carried out for standard map at $K = K_G$ when $\rho \approx 1$ (Fig. 5). Finally, in Ref. [17] the same value $\rho = 2$ was obtained taking account of all the internal borders, assuming a universal dependence $P(\tau)$ at any chaos border.

Let us take a different approach to this problem. Suppose the transition time of a trajectory between neighbouring scales

$$\tau_n \sim q_n^k. \quad (6.3)$$

Then, the numerical value $\rho_c \approx 1/2$ and relation $\mu_n \sim q_n^{-2}$ imply that

$$k = 4. \quad (6.4)$$

How could one explain such a big k value? It is clear, first of all,

that value (6.4) cannot characterize the renormalization attractor itself on which the scaling for any time is given by eq. (6.1), whence $\tau_n/\tau_{n-2} \sim s^2$, and $k=1$.

We conjecture that the statistical properties of the chaotic motion with a border are determined not by the renormalization dynamics on the attractor but rather by deviations from this dynamics at finite n . If eq. (6.3) with $k > 1$ describes the convergence to renormalization attractor then it should be $\tau_n = \infty$ on the attractor that is all the scales there are dynamically isolated.

Now, what determines the particular k value (6.4)? The following hypothesis was put forth in Ref. [21] (see also Ref. [19]). The convergence (6.3) is controlled by some effective local perturbation which generally depends on the distance to the chaos border. In separatrix map (1.1), for instance, such a perturbation could be characterized by the parameter

$$K(r) \approx K_g + F(r - r_g) \quad (6.5)$$

of the standard map (1.2) which locally (in z or r) describes the dynamics of map (1.1). The linear dependence seems to be typical for the chaos-order transition.

The empirical dependence (3.8) and (3.11) implies that perturbation (6.5) would destroy, at the one side of the border, only resonances with

$$q \geq Q_n \sim \frac{1}{|r_n - r_b|} \sim q_n^2. \quad (6.6)$$

These just form narrow ($\Delta r_s \sim Q_n^{-2} \sim q_n^{-4}$) chaotic layers between the principal scales, and, thus, determine the transition time τ_n . The latter can be roughly estimated as follows (see Ref. [19]). The diffusion rate in the narrow layer $D_n \sim Q_n^{-4} \cdot Q_n^{-1} \sim Q_n^{-5}$. The gradient of distribution function $f_n \sim q_n^2$ over the layer width $\sim Q_n^{-2}$ is of the order $\nabla f_n \sim q_n^2 Q_n^2$. Hence, the flux

$$\tau_n^{-1} \sim D_n \nabla f_n \sim Q_n^{-5} q_n^2 Q_n^2 \sim \frac{q_n^2}{Q_n^3} \sim q_n^{-4} \quad (6.7)$$

and we arrive at estimate (6.3) with the required value of $k=4$.

This mechanism appears to be typical for the chaos-order transition. It is natural to assume that the chaos-chaos transition corresponds to the special case of $F=0$ in eq. (6.5). If, for example, $\Delta K \sim (\Delta r)^l$ then, similarly to the above estimates, we obtain

$Q_n \sim (\Delta r)^{-l} \sim q_n^{2l}$, and from eq. (6.7)

$$\tau_n \sim \frac{Q_n^3}{q_n^2} \sim q_n^{2(3l-1)}. \quad (6.8)$$

Hence, $k=6l-2$, and $p_c = (3l-1)^{-1}$. Particularly, for $l=2$ we have $k=10$, and $p_c=1/5$.

Unfortunately, the latter approach is also not free of some contradictions. In particular, numerical data in Ref. [26] on the dependence $r_b(K)$ for standard map appear to suggest that $l=1/2$, and we come back to the case (6.1), (6.2) which is impossible to reconcile with our numerical results on $P(\tau)$.

The most direct method for studying the statistical anomalies would be a straightforward measurement of the exponent k in eq. (6.3). We mention also that for $k > 2$ the effect of internal chaos border could be neglected. The latter case was missed in Ref. [17].

7. CONCLUDING REMARKS

Even though the whole critical structure occupies a negligible part of the phase plane along a chaos border it is just this structure which determines some statistical properties of the whole chaotic component of motion. The most important of those properties is a power law decay of correlations with the exponent $p_c \approx 0.5 < 1$. First of all, this results in a singular motion spectrum («power spectrum») at $\omega \rightarrow 0$ [19]:

$$S(\omega) \sim \omega^{p_c-1} \sim \omega^{-1/2}. \quad (7.1)$$

Moreover, if such a slow decaying correlation determines the diffusion in another freedom, its rate proves to be abnormally fast [21]:

$$\sigma^2 \sim t^{2-p_c} \sim t^{3/2}, \quad (7.2)$$

where σ^2 is the dispersion of the distribution function. An interesting problem is the complete statistical description of such a superfast diffusion.

To what extent these anomalies do persist in a many-dimensional system? Thus far, this question remains open although a possibility was mentioned in the first paper [24] to generalize the renormalization group onto the many-dimensional case.

One of the most intriguing results in studying of critical phenomena in dynamics was the discovery of a new type of dynamical chaos, the renormalization chaos (Section 4). A similar phenomenon was briefly mentioned in Ref. [31] in connection with deviations from Kolmogorov's spectrum of turbulence, and in Ref. [32] on the models of spin glasses. However, the most impressing example of the renormalization chaos, which as a matter of fact has been known already since long ago, is the chaotic oscillation of the metrics in homogeneous but anisotropic cosmological models [33] (for recent results see Ref. [34]).

We express our sincere gratitude to F. Vivaldi, who attracted our attention to the critical phenomena in dynamics for important additional numerical data, to D. Escande for most helpful stimulating discussions, and to V.I. Arnold, L.A. Bunimovich, P. Grassberger, J. Greene, K.M. Khanin, I. Percival, D.V. Shirkov, and Ya.G. Sinai for valuable comments. We are also indebted to L. Kadanoff, and R. MacKay for informing us on their results prior to publication.

REFERENCES

1. *Alekseev V.M. and Yakobson M.V.* Phys. Reports, 1981, v.75, p.287.
2. *Alder B.J. and Wainwright T.E.* Phys. Rev. Lett., 1967, v.18, p.988.
3. *Reichl L.E.* A Modern Course in Statistical Physics. Austin: University Press, 1984.
4. *Bunimovich L.A.* Zh. Eksp. Teor. Fiz., 1985, v.89, p.1452.
5. *Chirikov B.V.* Phys. Reports, 1979, v.52, p.263.
6. *Lichtenberg A.J., Lieberman M.A.* Regular and Stochastic Motion, B., Springer, 1983.
7. *Chirikov B.V., Shepelyansky D.L.* Proc. 9th Intern. Conf. on Nonlinear Oscillations (Kiev, 1981). Kiev: Naukova Dumka, 1983, v.2, p.421. English translation available as PPL-TRANS-133, Plasma Physics Lab., Princeton University, 1983.
8. *Channon S.R. and Lebowitz J.L.* Ann. N.Y. Acad. Sci., 1980, v.357, p.108.
9. *Karney C.F.F.* Physica D, 1983, v.8, p.360.
10. *Greene J.M.* J. Math. Phys., 1968, v.9, p.760; 1979, v.20, p.1183.
11. *MacKay R.S.* Physica D, 1983, v.7, p.283.
12. *Shenker S.J. and Kadanoff L.P.* J. Stat. Phys., 1982, v.27, p.631.
13. *MacKay R.S., Meiss J.D. and Percival I.C.* Physica, D, 1984, v.13, p.55.
14. *MacKay R.S. and Percival I.C.* Comm. Math. Phys., 1985, v.98, p.469.
15. *Escande D.F.* Phys. Rep., 1985, v.121, p.163.
16. *Escande D.F. and Doveil F.* J. Stat. Phys., 1981, v.26, p.257.
17. *Chirikov B.V.* Lecture Notes in Physics, 1983, v.179, p.29.
18. *Greene J.M. and MacKay R.S.* Phys. Lett. A, 1985, v.107, p.1.
19. *Chirikov B.V.* Proc. Intern. Conf. on Plasma Physics, Lausanne, 1984, v.2, p.761.
20. *Arnold V.I.* Usp. Mat. Nauk, 1963, v.18, N 6, p.91.

21. *Chirikov B.V. and Shepelyansky D.L.* Physica D, 1984, v.13, p.395.
22. *Ostlund S., Rand D., Sethna J. and Siggia E.* Physica D, 1983, v.8, p.303.
23. *Kornfeld I.P., Sinai Ya.G., Fomin S.V.* Ergodic Theory. M.: Nauka, 1980 (in Russian).
24. *Rand D., Ostlund S., Sethna J. and Siggia E.* Phys. Rev. Lett., 1982, v.49, p.132.
Farmer J.D. and Satiya I.I. Phys. Rev. A, 1985, v.31, p.3520.
Farmer J.D. and Umberger D.K. Phys. Lett. A, 1986, v.114, p.341.
25. *Grassberger P.* Private communication, 1985.
26. *Greene J.M., MacKay R.S. and Stark J.* Physica D, 1986, v.21, p.267.
27. *Hanson J.D., Cary J.R. and Meiss J.D.* J. Stat. Phys., 1985, v.39, p.327.
28. *Vivaldi F.* Private communication, 1985.
29. *Cassel J.W.S.* An Introduction to Diophantine Approximation. Cambridge Univ. Press, 1957.
30. *Meiss J.D. and Ott E.* Phys. Rev. Lett., 1985, v.55, p.2741.
31. *Frisch U.* Chaotic Behaviour of Deterministic Systems. Les Houches 1981. Amsterdam, North-Holland, 1983, p.665.
32. *McKay S.R., Berker A.N. and Kirkpatrick S.* Phys. Rev. Lett., 1982, v.48, p.767.
33. *Landau L.D., Lifshitz E.M.* Field Theory. M.: Nauka, 1973.
34. *Lifshitz E.M., Khalatnikov I.M., Sinai Ya.G., Khanin C.M., Schur L.N.* Pis'ma Zh. Eksp. Teor. Fiz., 1983, v.38, p.79.
35. *Satiya I.I.* Phys. Rev. Lett., 1987, v.58, p.623.

B.V. Chirikov and D.L. Shepelyansky

Chaos Border and Statistical Anomalies

Б.В. Чириков, Д.Л. Шепелянский

Граница хаоса и статистические аномалии

Ответственный за выпуск С.Г.Попов

Работа поступила 26 июня 1986 г.

Подписано в печать 5.12 1986 г. МН 11883.

Формат бумаги 60×90 1/16 Объем 2,0 печ.л., 1,6 уч.-изд.л.

Тираж 180 экз. Бесплатно. Заказ № 45

*Набрано в автоматизированной системе на базе фото-
наборного автомата ФА1000 и ЭВМ «Электроника» и
отпечатано на ротапринтере Института ядерной физики
СО АН СССР,
Новосибирск, 630090, пр. академика Лаврентьева, 11.*